RSC Advances

PAPER

View Article Online
View Journal | View Issue

Cite this: *RSC Adv.*, 2025, **15**, 11023

Preparation of chitosan/polyvinyl alcohol/white round grapefruit essential oil and polyethylene terephthalate films for *Lycium barbarum* preservation†

Mengyun Liu,[a] Liuxin Shi, *[a] Xiao Zhang[a] and Yunfeng Zhang[b]

This study aimed to produce bilayer films spiked with white round grapefruit essential oil and apply them to preserve *Lycium barbarum*. A chitosan/polyvinyl alcohol film doped with white round grapefruit essential oil was prepared as an inner film, and a polyethylene terephthalate film was prepared as an outer film through a solution casting method. The volatile compounds of white round grapefruit essential oil (87.5573%), mainly D-limonene (34.389%), *cis*-*p*-mentha-2,8-dien-1-ol (5.154%), *trans*-carveol (5.148%), limonene oxide, *cis*-β-ocimene (4.892%) and *trans*-β-ocimene (4.130%), were identified through gas chromatography-mass spectrometry and found to have strong antimicrobial activities against *Escherichia coli*, *Staphylococcus aureus*, and *Aspergillus niger*. The addition of white round grapefruit essential oil to the chitosan/polyvinyl alcohol film resulted in a significant improvement in the flexibility and antimicrobial properties of the films; the thermomechanical properties were more stable; however, the film water content and soluble solid content changes were not significant. The double-layer film was applied in the preservation of *Lycium barbarum*, and results showed that the double-layer film effectively reduced the water loss rate, decay rate, malondialdehyde content, and color change of *Lycium barbarum* compared with the control group and prolonged the shelf-life of *Lycium barbarum*.

Received 26th December 2024
Accepted 17th March 2025

DOI: 10.1039/d4ra09018g

rsc.li/rsc-advances

1. Introduction

Traditional packaging, which is dominated by petroleum-based plastics, considerably burdens the environment, and there is an increasing emphasis on the use of environmentally friendly bio-based films.[1,2] Chitosan (CS) is the second most abundant natural polymer, after cellulose, and is a polysaccharide derived from chitin. It is considered one of the most promising polymers.[3] CS films offer semi-permeability, flexibility, and natural antimicrobial properties comparable to some commercial polymers. It is widely employed in various industries such as coatings, food, agriculture, textiles, and wastewater treatment.[4] However, the large particle size of CS and the poor oxygen barrier performance after film formation have limited the application of a single film. Therefore, it is often blended with other polymers, among which polyvinyl alcohol (PVA) was chosen for its excellent film-forming properties, oxygen barrier, and degradability.[5] Some scholars have mixed it with CS to prepare films for applications in functional packaging materials, pharmaceuticals, and food packaging.[6,7]

For food packaging materials, antimicrobial properties are a prerequisite for preventing bacterial and fungal contamination of food. However, the antimicrobial properties of a single CS are limited, and other antimicrobial substances must be added. Essential oils, known for their potent antimicrobial properties and safety, are garnering attention in this context.[8] They are favored in the food industry for their antioxidant, antimicrobial, and non-toxic properties and are used for a variety of purposes, including blending into film-forming substrates for packaging fruits, vegetables, and meat products, microencapsulating to prolong the storage period of dairy products, infusing into air-conditioned packaging to improve the shelf life of grain products, and combining with electrostatic spinning in film preparation for meat product storage.[9] Yang *et al.* prepared a chitosan/carboxymethyl jellied gel composite film with added mustard essential oil to extend the storage time of mango.[10] Therefore, blending essential oils into films can enhance their biological and physical properties, which is positive for food preservation. White grapefruit essential oil (WEO) contains a large number of hydrophobic groups and limonene, which contribute to its film barrier and antimicrobial properties. However, no antimicrobial evaluation of WEO has been reported to date.

[a]*College of Light Industry and Food Engineering, Nanjing Forestry University, Nanjing 210037, China*

[b]*Hangzhou Ruili Ultrasound Technology Co., Ltd., Hangzhou, Zhejiang, 310024, China*

† Electronic supplementary information (ESI) available. See DOI: https://doi.org/10.1039/d4ra09018g

At present, pure bio-based films exhibit limited antimicrobial and barrier properties. They can be used in combination with a polyethylene terephthalate film (PET). Li *et al.* prepared a double-layered smart film of konjac glucomannan/carmine/keratine gum containing oregano essential oil, which was biodegradable but had relatively poor moisture and oxygen barrier properties.[11] In high humidity environments, the films tend to absorb moisture and become sticky, which can affect their usability and preservation; and they cannot effectively inhibit the growth of aerobic microorganisms and oxidative reactions of food, which can shorten the shelf life of food.[12] Many biodegradable double-layer films exhibit weaker strength, flexibility, and tensile strength than traditional non-biodegradable plastic films, making them susceptible to damage and tearing during packaging, transportation, and storage, which can lead to contact between the food and the external environment, compromising preservation. In this research, the above-mentioned problems were overcome by adding PET to the outer film, and PET can be reused, which reduces the pressure on the environment to a certain extent.

Bilayer film technology is proving to be an effective way to protect natural active substances in packaging films. To date, bilayer film technology has not been used to develop packaging films based on white round grapefruit essential oil. In this study, bilayer films loaded with white round grapefruit essential oil were prepared for evaluating the freshness of fresh goji berries (*Lycium barbarum*). The inner film is a CS/PVA film doped with white round grapefruit essential oil: the presence of essential oil gives excellent antibacterial properties and CS/PVA composite films act as carriers for essential oils; the outer film is a high-barrier PET film. Fresh goji berries are rich in nutrients, but storage and transportation are difficult due to their high respiratory activity after harvesting.[13] Existing methods usually dehydrate the berries to produce dried fruit or juice, but they lose their nutritional value.[14] Therefore, the development of packaging materials with strong freshness preservation and environmental friendliness is necessary.

2. Materials and methods

2.1 Materials

Chitosan, with a deacetylation level of 80–95%, was procured from Shanghai Sinopharm Chemical Reagent Co., Ltd. PVA was obtained from Shanghai Macklin Biochemical Co., Ltd, while PET was sourced from Hengli Group. Wolfberry was acquired from Zhongning, Ningxia, and the white round grapefruit was purchased from a vegetable market in Nanjing. *Escherichia coli* CMCC(B) 44102, *Staphylococcus aureus* CMCC(B) 26003, and *Aspergillus niger* CMCC(F) 98003 were obtained from Nanjing Lezhen Biotechnology Co.

2.2 White round grapefruit essential oil extraction

WEO was extracted by steam distillation. White round grapefruit peels were cleaned and dried at 35 °C, and then crushed. A three-necked flask was filled with distilled water at the bottom, and the finely crushed peels (wrapped in gauze at the bottom) were placed in the distillation flask. A condensing unit is connected to a heating unit, and water is heated and boils to produce steam, which rises to distill the raw material. The distillation time is 8 h. Finally, the essential oils were eluted from the walls of the condenser tube with acetone and separated. The extracted essential oils were stored at a low temperature away from light (the diagram of the experimental setup is presented in the ESI†).

The composition and stereochemical configurations of white round grapefruit essential oil were analyzed using an Agilent 7890A + 5975C chromatography-mass spectrometry (GC-MS) instrument with the following analytical parameters: DB-5MS column (30 m × 0.25 mm × 0.25 μm), 1 μL injection volume and 50 : 1 separation mode (v/v). Carrier gas was helium (99.999% purity, 1 mL min^{-1}). The temperature of the injector was set at 280 °C. The oven temperature was initially set at 40 °C and held for 52 min; then it was gradually increased to 270 °C at 5 °C min^{-1} and held for 22 min. Reference conditions for mass spectrometry: ion source temperature = 230 °C; quadrupole temperature = 150 °C; transmission line temperature = 280 °C; ionization mode = EI; solvent delay time = 1 min; data acquisition mode = full-scan mode; mass-to-charge ratio (m/z) = 35–550 amu. A total of 50 compounds were identified (87.5573%): D-limonene (34.389%), *cis-p*-mentha-2,8-dien-1-ol (5.154%), *trans*-carveol (5.148%), limonene oxide, *cis*-β-ocimene (4.892%), and *trans*-β-ocimene (4.130%). A total of 23 chiral compounds were detected (detailed information is provided in the ESI†).

2.3 Preparation of the composite films

CS (2% w/v) was dissolved in a glacial acetic acid (1% v/v) solution for 2 h, and PVA (3% w/v) was dissolved in deionized water at 72 °C for 1 h. The two solutions (CS and PVA, 1 : 1, v/v) were mixed for 30 min, glycerol (10% w/w of CS and PVA) was added and mixed for 30 min, and then, the mixture was homogenized for 4 min in a cell crusher. Following this, 1% v/v white round grapefruit essential oil and 0.8 g of Tween-80 were added and homogenized for 5 min until the essential oil was completely dissolved. After defoaming the mixed solution, 20 g and 15 g of the film solution were taken, respectively, poured evenly into the polytetrafluoroethylene mold and PET film, and dried at 30 °C for 3 h. Finally, the prepared film should be equilibrated at 50% relative humidity. The wolfberries were divided into two groups: unpacked (Control) and double-laminated film-packed (CPWP) (as shown in Fig. 1).

2.4 Investigation of the antimicrobial activity

For antimicrobial tests, *Escherichia coli*, *Staphylococcus aureus*, and the goji berry pathogen *Aspergillus niger* were selected. Bacteria were cultured on an LB solid medium, and the inhibitory activity was evaluated using the circle of inhibition method. First, 100 μL of bacterial suspension was added before the solidification of the LB medium. After solidification, the sterilized membrane disk was briefly immersed in the sample (essential oils and film-forming solutions) and then placed on the bacteria-containing plate, with two disks per plate. Acetone

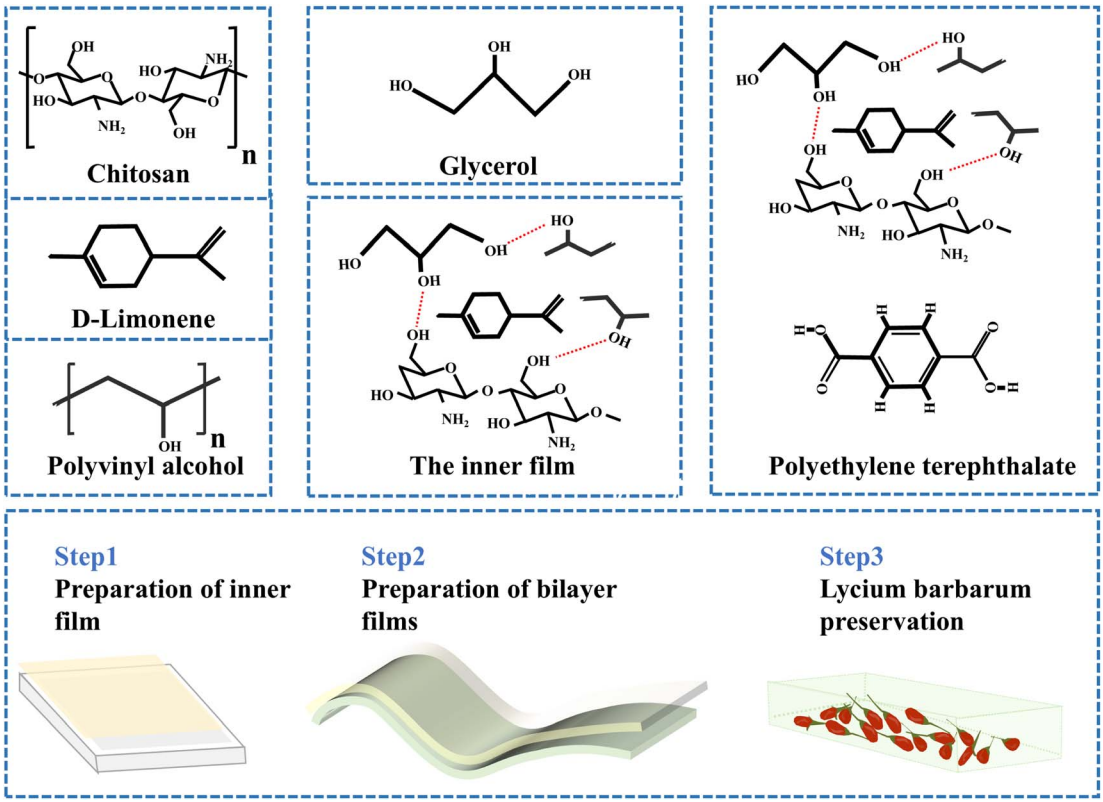

Fig. 1 Graphical abstract of double-layer film application for the preservation of *Lycium barbarum*. CPW refers to the chitosan/polyvinyl alcohol/white round grapefruit essential oil film. CPWP refers to the chitosan/polyvinyl alcohol/white round grapefruit essential oil and polyethylene terephthalate films.

served as the control. The inhibition circle's diameter was measured at 37 °C after 24 h of incubation. Fungi were cultured on solid PDA plates, and their inhibitory activity was assessed using the diffusion method. Fungal suspensions were spread on a solidified PDA medium, 6 mm diameter Oxford cups were placed, white round grapefruit essential oil was added, and acetone was used as the control. The diameters of the inhibition circles were measured at 28 °C after 48 h of incubation.

2.5 Characterisation of the films

2.5.1 Fourier transform infrared (FTIR) spectroscopy determination. The chemical structure analysis of the film-forming material was performed in attenuated total reflection mode using a Fourier-transform infrared spectrometer (Germany, Bruk, VERTEX 80V), with spectral recordings in the range of 4000–500 cm^{-1} with a resolution of 4 cm^{-1}.

2.5.2 X-ray diffraction (XRD) analysis. Film samples (2 cm × 2 cm) were analyzed using an XRD (Japan, Rigaku, XRD Ultima IV) with a diffraction angle of 2θ in the scanning range of 10–90° at a scanning rate of 5° min^{-1}.

2.5.3 Scanning electron microscopy (SEM) analysis. A scanning electron microscope (America, FEI, Quanta) was used to study the microstructure of the polymer films, and the sample was plated on aluminum stubs and sputter-coated (EMS Quorum 150 TES, USA) with a 25 nm platinum layer before scanning. Multiple magnifications and imaging parameters were used, including a 5 kV voltage, 3.5 nm spot size, 30 μm objective aperture, and 8 mm working distance.

2.5.4 Thermogravimetric analysis. The thermal degradation of the polymer films was analyzed using a TGA209 F1 thermogravimetric analyzer, with measurements taken at an airflow rate of 50 mL min^{-1} in the temperature range of 30–600 °C at a heating rate of 10 °C min^{-1}.

2.5.5 Thickness. The thickness of the films was determined by measuring the distance using a calibrated micrometer with a sensitivity of 0.001 mm. Ten random locations on the sample were selected for the measurement.

2.5.6 Mechanical properties. The films were tested using an electronic universal testing machine to measure the elongation at break (EB) and tensile strength (TS). Samples were rectangular (150 mm length, 20 mm width). The tests were performed at 25 °C, the instrument speed was controlled at 100 mm min^{-1}, and the initial distance was 50 mm.

2.5.7 Oxygen (OP) and water vapor barrier properties (WVP). WVP was measured at 25 °C and 90% RH. The oxygen transmission rate was determined using a differential pressure gas permeation meter at an ambient temperature of 25 °C and 50% RH.

2.5.8 Water contact angle (WCA). A video-equipped contact angle meter was used to measure the WCA. The films were affixed to a glass slide, and 4 μL of deionized water was slowly dripped onto the film surface over 10 s. The WCA was calculated

using the instrument's software based on the water droplet's shape on the film surface at equilibrium.

2.5.9 Moisture content (MC) and total soluble matter (TSM). The method of determining the MC of the films was modified slightly by the approach proposed by Lamarra *et al.*[15] The film samples were divided into 2.5 cm × 2.5 cm squares, and the initial weight (M_1) was recorded. Subsequently, it was dried at 105 °C until a constant weight was achieved. This was then reweighed (M_2). MC was calculated based on eqn (1):

$$\mathrm{MC}(\%) = \frac{M_1 - M_2}{M_1} \times 100\%. \quad (1)$$

Following drying, the film was immersed in distilled water at room temperature for five days. During this period, the water was replaced daily. Thereafter, the film was dried to a constant weight at 50 °C (M_3). The TSM content was calculated based on eqn (2):

$$\mathrm{TSM}(\%) = \frac{M_2 - M_3}{M_2} \times 100\% \quad (2)$$

2.5.10 Color. Film color was measured using a ZB-B whiteness meter, assessing L^* (brightness), a^* (redness), and b^* (yellowness), and calculating ΔE^* based on eqn (3):

$$\Delta E^* = \sqrt{(\Delta L^*)^2 + (\Delta a^*)^2 + (\Delta b^*)^2}. \quad (3)$$

2.6 Preservation of wolfberry

2.6.1 Weight loss (WL) and decay weight (DW). The loss in weight of the wolfberry (%) was determined using eqn (4):

$$\mathrm{WL}(\%) = \frac{m_1 - m_2}{m_1} \times 100\% \quad (4)$$

where m_1 is the initial weight at the beginning of the storage period and m_2 is the weight at the end of the storage period.

The weight of decayed fruit (%) was determined using eqn (5):

$$\mathrm{DW}(\%) = \left[\sum \frac{(a \times b)}{(N \times A)}\right] \times 100\%. \quad (5)$$

where a is the category of rot intensity, b is the frequency of rot occurrence, N is the total number of examined fruits (healthy and infected), and A is the highest category of decay intensity observed.

2.6.2 Solid soluble (TSS) and titratable acidity (TA) content. The TSS content of *Lycium barbarum* was measured using a handheld digital refractometer and expressed as Brix. The TA content was measured by titrating with 0.1 M NaOH, and the acid in wolfberry was converted into malic acid.[16,17]

2.6.3 Malondialdehyde (MDA) content. MDA in wolfberry was determined by adding 10 mL of TCA solution (100 g L^{-1} trichloroacetic acid) to 1.0 g of wolfberry pulp, grinding it into a homogenate, and freezing, followed by centrifugation at 4 °C and 10 000 rpm min^{-1} for 20 min. Subsequently, 2 mL of TBA solution (0.67% thiobarbituric acid) was added to 2 mL of the supernatant, boiled at 100 °C for 20 min, cooled down, and centrifuged. The absorbance was measured at 600 nm, 532 nm, and 450 nm using a 2 mL mixture of TCA and 2 mL of TBA as the control.[18]

$$C\ (\mu\mathrm{mol\ L^{-1}}) = 6.45 \times (\mathrm{OD}_{532} - \mathrm{OD}_{600}) - 0.56 \times \mathrm{OD}_{450} \quad (6)$$

$$\mathrm{MDA}(\mu\mathrm{mol\ g^{-1}}) = \frac{C \times V}{V_s \times m \times 1000} \quad (7)$$

where C is the malondialdehyde content of the reaction mixture, where C is the malondialdehyde content of the reaction mixture, V is the volume of the sample extract, V_S is the volume of the extract at measurement, and m is the mass of the fruit sample.

2.6.4 Relative electrolytic leakage (REL). The cell membrane permeability measurement method was modified.[19] REL was determined by weighing 3.0 g of the fruit pulp. The samples were submerged in 30 mL of distilled water, and the initial conductivity was measured after one hour. The samples were then boiled for ten minutes, cooled to room temperature, replenished with distilled water to the original weight, and the final conductivity was measured.

$$\mathrm{REL}(\%) = \frac{a_1 - a}{a_2 - a} \times 100\% \quad (8)$$

where a_1 is the initial conductivity, a_2 is the final conductivity, and a is the conductivity of distilled water.

2.7 Statistical analysis

Experimental data are presented as mean ± standard deviation and graphed using Origin 2025. One-way analysis of variance (ANOVA) was used to assess significant differences, with statistical significance defined as $p < 0.05$.[20–22]

3. Results and discussion

3.1 Investigation of the antimicrobial activity

The inhibitory activities of the extracted white round grapefruit essential oil and films against the tested bacteria are illustrated in Fig. 2. White round grapefruit essential oil exhibited a high inhibitory activity (>16 mm) against *Escherichia coli*, *Staphylococcus aureus*, and *Aspergillus niger*. Notably, against *Aspergillus niger*, the causative agent in *Lycium barbarum*, the diffusion inhibition distances reached up to 22 mm. Essential oils are a class of plant secondary metabolites, mainly composed of volatile aromatic extracts, among which aldehydes, phenols, and oxygenated terpenes are the main antibacterial active substances. The active ingredients in these substances can disrupt the permeability of cell membranes, resulting in the inability to synthesize genetic materials and proteins within the cell, thereby hindering the formation of bacterial cells and exerting antimicrobial effects. White round grapefruit essential oil was identified by GC-MS to inhibit fungal growth through synergistic or antagonistic effects.[1,2] Monoterpenes inhibit fungal growth by increasing the lipid peroxide concentrations, which leads to cell death.[3] The antibacterial capacity of a single CS film is limited; after the addition of white round grapefruit

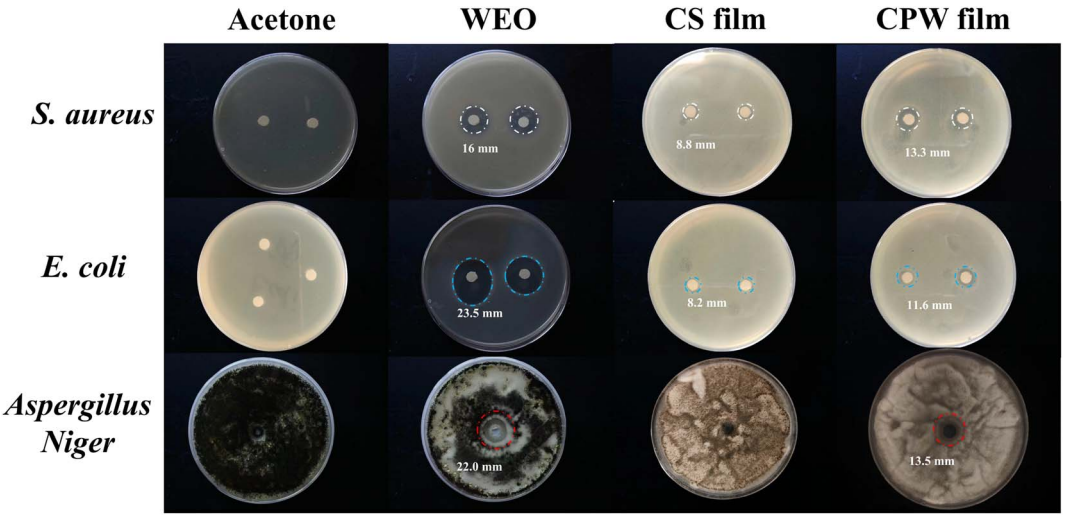

Fig. 2 Antibacterial properties of the essential oil and different films.

essential oil, the inhibition zone diameter against *Escherichia coli* reached 11.6 mm, that against *Staphylococcus aureus* reached 13.3 mm, and that against *Aspergillus niger* reached 13.5 mm. The results showed that the addition of essential oils enhanced the antimicrobial properties of the film.

3.2 FT-IR spectroscopy and XRD

The FTIR spectrum analyzed the characteristic absorption of infrared radiation at different wavelengths and identified specific functional groups. Fig. 3(a) shows the FITR spectral variations of each component between the films. The characteristic peaks of white round grapefruit essential oil also appeared in CPW, specifically at 2900 cm^{-1} (C–H stretching vibration), 1600 cm^{-1} (C=C stretching vibration), 1400 cm^{-1} (C–H bending vibration), and 1350 cm^{-1} (C–O–H stretching vibration). In the CPW film, the vibrational absorption of the C–O bond in alcohols, ethers, or esters is observed at 1028 cm^{-1}. The peak at 2895 cm^{-1} corresponds to the C–H stretching. This indicates that the essential oil has been successfully loaded into the film.[23,24] The CS film exhibits characteristic bands at 3434 cm^{-1} (–OH and –NH stretching vibrations), 1658 cm^{-1} (amide I C=O stretching vibration), 1428 cm^{-1} (–OH stretching vibration), and 1101 cm^{-1} (C–O–C bridge and C–O asymmetric stretching vibrations).[25,26] PVA shows –OH stretching vibrations and main chain aliphatic C–C bending vibrations at 3419 cm^{-1}, 2838 cm^{-1}, and 1175 cm^{-1}. Due to the formation of hydrogen bonds, the band at 3303 cm^{-1} in the CPW film broadens and the characteristic peak at 1545 cm^{-1} shifts to 1550 cm^{-1}, indicating interactions between the amino groups of CS and PVA and the essential oil.[27]

The XRD analysis of CPW and CPWP is shown in Fig. 3(b); typically CS shows spikes at 18–20° and PVA at both 18–20° and 40°.[28] The crystallinity of CPW is reduced compared to pure CS and PVA. Because the PVA and CS molecules are completely intertwined with each other, the arrangement rules between the PVA and CS molecules are severely disrupted by themselves, resulting in a decrease in crystallinity.[29] After applying CPW to the PET film, the crystallinity of the composite film increased from 74.49% to 76.29%. This may be because the molecular chains are arranged in the direction of stress during the drying process, which is conducive to the occurrence and development of crystallization, and thus improves the crystallinity.

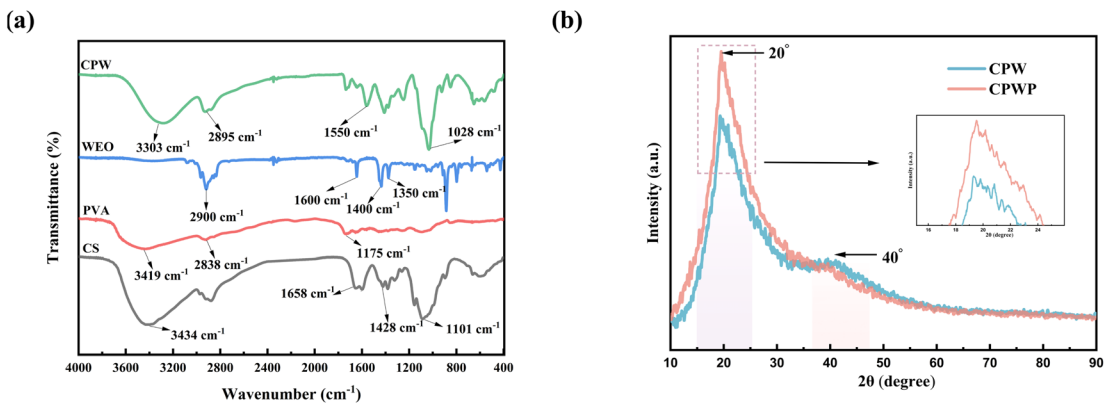

Fig. 3 (a) FTIR spectra and (b) XRD patterns of the films.

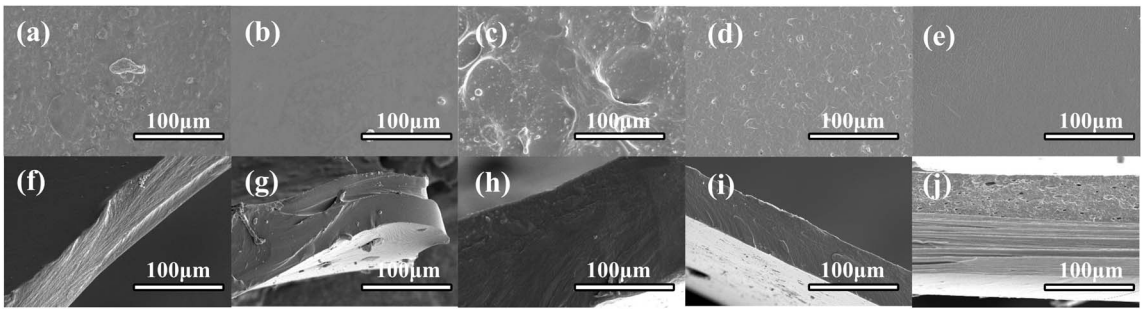

Fig. 4 (a) CS, (b) PVA, (c) CS/PVA, (d) CPW, and (e) CPWP film surfaces. (f) CS, (g) PVA, (h) CS/PVA, (i) CPW, and (j) CPWP film cross-section surfaces.

3.3 SEM

The microstructural results of the films are presented in Fig. 4(a–j). The surface cross-section of the CS film was uneven and rough, while the surface of the PVA film was smooth and continuous. The surface and cross-section of the CS/PVA film were continuous, indicating that CS and PVA were miscible and had good compatibility. The addition of white round grapefruit essential oil to the composite film resulted in voids and bubbles on the film surface. This was due to the evaporation of water from the film during drying and the migration of the essential oil to the surface of the polysaccharide network for further evaporation. A similar phenomenon was observed by Erceg *et al.*[30] in cellulose acetate films. The CS/PVA coatings on PET films with essential oils appeared to have a smoother surface with reduced porosity and tightly aligned cross sections with no delamination.

3.4 TGA and DTG

TGA was employed to assess the thermal stability of the materials. Fig. 5(a–d) shows the TGA and DTG (first-order derivative of the TGA curve) images of the samples; the thermal degradation of the CS film is divided into three stages, the PVA film is divided into two stages, whereas WEO is divided into only one stage, and CPW shows a multistage decomposition process. The

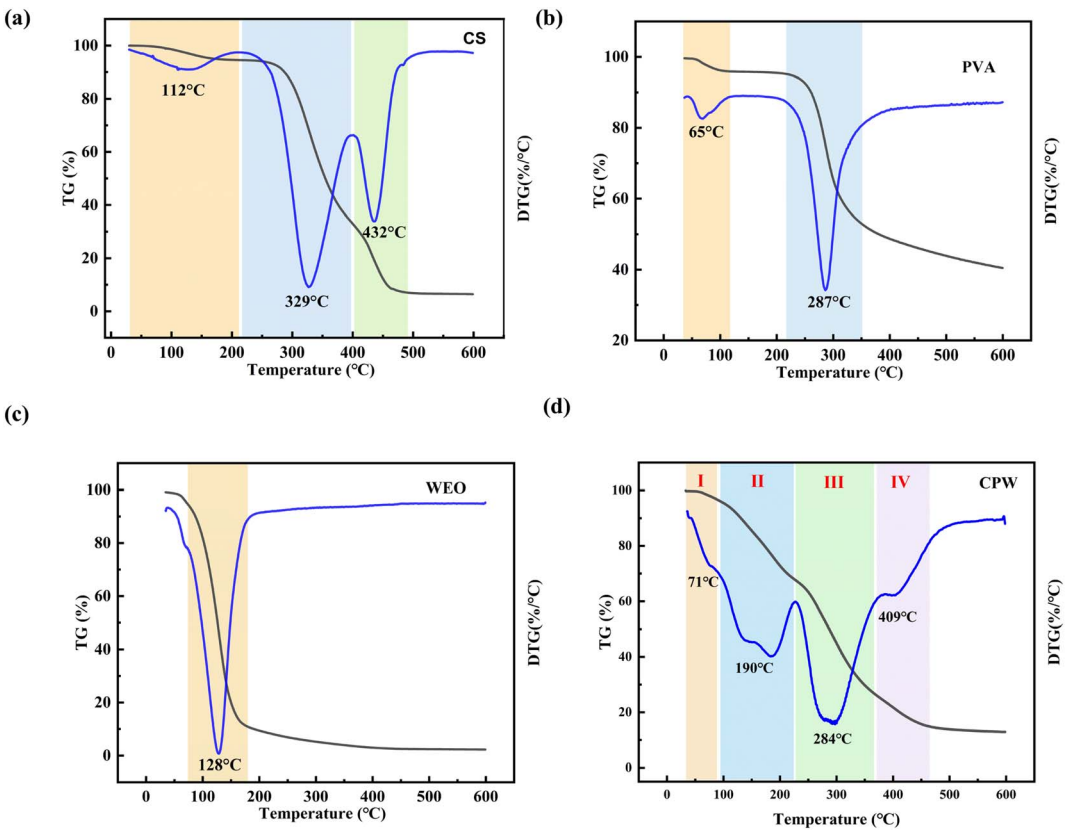

Fig. 5 TGA and DTG thermograms of (a) CS film, (b) PVA film, (c) WEO, and (d) CPW.

Table 1 Thermal parameters of the film

Samples	T_0 (°C)	T_{max} (°C)
CS	252	329
PVA	215	287
WEO	80	128
CPW	225	284

initial mass loss (30–108 °C) is associated with the evaporation of water from the film; the second stage (117–226 °C) is associated with the decomposition of glycerol and matrix in the film, the third stage (227–365 °C) is the decomposition of polymers in the film, and the final stage (377–454 °C) is the decomposition of high-temperature stabilizing substances in the film. The highest thermal degradation of the film was at the third-stage temperature of 270 °C. Overall, the thermal stability of the film was improved (Table 1).

3.5 Mechanical and thickness properties

Fig. 6(a) illustrates the thickness of the films. The incorporation of PVA and essential oils in the film solution, at equal mass, increased the thickness. Wang *et al.* found that cinnamon essential oils resulted in a greater thickness of CS-based films, possibly due to some film solution escaping during the drying process, creating pores and thus increasing thickness.[31] TS represents the cohesion force between polymers in the film, while EB denotes the film's elasticity before fracture.[32] Compared to pure CS films, the addition of PVA increased the tensile strength of the films from 22.12 ± 0.43 MPa to 32.02 ± 0.62 MPa. The addition of WEO further increased the tensile strength of the films to 48.23 ± 0.65 MPa. However, the elongation at the break of the composite films showed a decreasing trend. This is similar to the results observed by Bispo *et al.*,[33,34] where the incorporation of essential oils into the films enhanced the interfacial interactions, thereby improving their mechanical properties.

3.6 WVP and OP

WVP refers to the rate of water vapor transmission through the film, which is a critical measure of the film barrier performance. Water vapor significantly affects the quality of packaged products. Stringent WVP standards are essential for dried fruit packaging, while fruits and vegetables benefit from lower WVP, as optimal humidity levels prevent water vapor condensation inside the package, aiding in product preservation.[35] Fig. 6(b) illustrates the WVP of the films. Incorporating essential oils is shown to reduce water vapor transmission, a result of the essential oils impeding moisture binding and complicating the moisture diffusion path.

OP assesses the film's ability to resist oxygen transmission, which is another key indicator of barrier efficacy. Adding PVA significantly lowers the OP of CS-based films, primarily due to PVA's excellent oxygen barrier properties. Further, introducing essential oils decreases the OP value of these films. PET is inherently a high-barrier material, and coating it with a chitosan-based film enhances its barrier performance, meeting the secondary standard for packaging materials.[35]

3.7 WCA

The contact angle represents the three-phase interfacial equilibrium among air, water, and the film, reflecting the film's surface characteristics.[36] The contact angles of the films are depicted in Fig. 6(c). The results indicate that the pure CS film has a hydrophilic nature with a contact angle of 56° ± 0.02°, primarily due to the hydroxyl groups in CS. Conversely, the inclusion of white round grapefruit essential oil increases the contact angle to 95.7° ± 0.01°, 41.67% ± 0.05% higher than that of pure CS, reducing the film's water sensitivity. This change is attributed to the hydrophobic properties of the essential oil.

3.8 MC, TSM, and color

In the context of microstructural film analysis, MC represents the total volume occupied by water molecules within the film, closely related to its micropores or pores (Table 2). TSM,

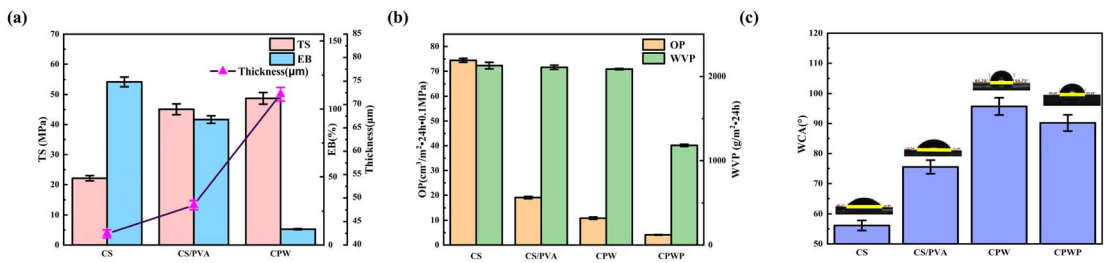

Fig. 6 (a) TS and EB, (b) OP and WVP, and (c) WCA of the films.

Table 2 MC, TSM, and color results of the films

Samples	MC (%)	TSM (%)	L^*	a^*	b^*	ΔE^*
CS	15.19 ± 0.67	12.50 ± 0.77	87.67 ± 1.87	−20.99 ± 0.88	25.55 ± 0.98	93.66 ± 1.80
CS/PVA	19.35 ± 0.76	35.00 ± 1.33	88.79 ± 1.88	−16.92 ± 0.80	26.45 ± 1.00	94.18 ± 1.82
CPW	14.29 ± 0.66	10.00 ± 0.71	86.05 ± 1.84	−13.92 ± 0.72	28.97 ± 1.04	91.86 ± 1.70

a crucial aspect of biodegradable films, is associated with the dissociation of hydrogen and ionic bonds and the ionization of amino and carboxyl groups. Incorporating essential oils into the film has led to decreased solubility, attributed to enhanced interactions between CS and the oils, consistent with the findings from the incorporation of lemon, thyme, and cinnamon oils into CS-based membranes.[37]

The higher the transparency of the film, the easier it is for consumers to make informed choices. Li *et al.* demonstrated that excessive film transparency can result in ultraviolet ray penetration, adversely affecting packaged products.[38] Tongnuanchan *et al.* illustrated that the inclusion of essential oil droplets in the film generates a light scattering effect, consequently reducing light transmittance and deepening the film's color.[39] This change in color correlates with the color of the white round grapefruit essential oil itself. Additionally, the presence of essential oils enhances the film's resistance to light, making it more suitable for packaging light-sensitive products.

3.9 Fruit appearance

The appearance of wolfberries packaged in the CPWP film is depicted in Fig. 7. The control group wolfberry fruits continued to shrink over time, with mold appearing on the 6th day and noticeable disease spots by the 13th day. In contrast, wolfberries packaged with the CPWP film exhibit minimal shrinkage, maintain a smooth and bright appearance, and show no disease spots at the end of storage. This improvement is attributed to the enhanced barrier and bacteriostatic properties of the CPWP film, which reduce the respiration rates and delay the peak of respiration, thereby extending the shelf life of the berries. Ebrahimi *et al.* observed similar results in guar bean-based film-coated preserved mangoes.[40]

3.10 WL and DW

Fruit weight loss primarily results from respiration and water evaporation. This loss is influenced by the atmospheric pressure and storage temperature. Fig. 8(a) illustrates the weight loss of wolfberries stored at 4 °C over 19 days. The water loss in all samples increased with the storage time. The control group exhibited consistently higher weight loss than the CPWP group, mainly due to factors such as carbon dioxide, water vapor, and oxygen. Packaging with the CPWP film reduced the exposure of the wolfberries to these elements, thereby reducing their weight loss. At the end of storage, the CPWP group showed a reduction

Fig. 7 Photographs of the appearance of wolfberry over time.

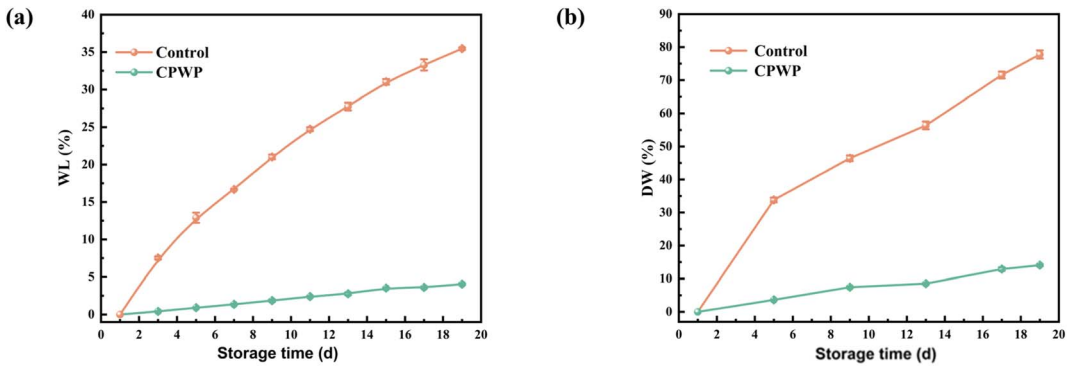

Fig. 8 (a) WL and (b) DW of wolfberries over time.

in weight loss of 88.15% ± 0.76% relative to the control group, primarily attributed to the superior moisture barrier properties of the double-layer film and the enhanced bacteriostatic effect of white round grapefruit essential oil, which maintained the quality of the goji berries. Roshandel-hesari *et al.* observed similar results with CS-based preservation of cherry tomatoes, where weight loss during storage was minimal, which was attributed to the high-barrier properties of PET films.[17]

The appearance of fruit significantly influences consumer purchase decisions, and decay is a major factor in postharvest losses of fruits and vegetables, accounting for approximately 60–70% of such losses.[41] Fig. 8(b) presents the decay rate of wolfberries during storage at 4 °C. Over time, the decay rate of both the control and CPWP groups gradually increased. The control group showed signs of rot by the fifth day of storage, with the rot intensity increasing to 70.83% ± 1.46% by the 17th day, leading to deterioration and an unpleasant odor, rendering the berries inedible. The rot rate of wolfberries in the CPWP group reached 13.88% ± 1.05% by the end of storage, but the fruits remained firm. Initial black spots appeared on the 13th day, indicating the exceptional antimicrobial properties of the bilayer film, effectively inhibiting decay. Yang *et al.* demonstrated that mustard essential oil can significantly reduce the decay rate of mango, effectively delaying its decay.[42]

3.11 TSS and TA

TSS comprises soluble sugars, acids, vitamins, minerals, and other soluble components in fruits, which are related to ripening, aging, and post-ripening processes and serve as vital indicators of fruit ripeness and flavor. Generally, a high WL is correlated with increased TSS, reflecting the fruit's ripeness. The changes in the soluble solid content of wolfberries during low-temperature storage are shown in Fig. 9(a). The results show that the TSS levels in both the control and CPWP groups increased over time, with the control group showing a more rapid increase. This trend is primarily due to the decomposition of fruit nutrients into monosaccharides and disaccharides during physiological metabolic processes. The CPWP group exhibited a slower TSS increase, attributed to the superior barrier effect of the double-layer film, which reduces the respiration rate of the fruit by restricting the gas exchange and thus prevents the drastic change in the TSS content.[43]

TA is a crucial parameter for evaluating the taste of fruit, with malic acid being the main component in the titratable acid content of wolfberry. Therefore, the TA of *Lycium barbarum* was measured using malic acid as the reference compound. Fig. 9(b) depicts the TA content of *Lycium barbarum* during low-temperature storage, revealing the following trends: the control group's TA initially decreased, then increased, reaching its peak on the 13th day, and decreased again. Conversely, the CPWP group's TA followed a similar pattern, peaking at 0.83% ± 0.09% on the 9th day, but overall exhibited a decreasing trend. Except for the 13th day, when the control group's TA was higher, the TA content in the CPWP group exceeded that of the control group at all other storage times. The decrease in TA reflects the changes in fruit metabolism caused by changes in organic acid composition during the respiratory process. Sogvar *et al.* demonstrated a similar decrease in the TA content in strawberries coated with aloe vera and ascorbic acid during storage.[44]

3.12 MDA and cell membrane permeability

MDA is a key indicator of lipid peroxidation and reflects the extent of cellular damage. It is positively correlated with fruit senescence, with the accumulation of MDA indicative of tissue damage.[45] Fig. 10(a) depicts the changes in MDA content in *Lycium barbarum* during low-temperature storage. The results indicate that the MDA levels increased in both the control and CPWP groups. However, the MDA content in the sample control was consistently higher than that of CPWP. By the end of the storage period, the MDA content in the CPWP decreased by 48.28% ± 0.47% compared to the control group. These findings suggest that CPWP can effectively reduce MDA accumulation and delay the senescence of *L. barbarum*. The findings of Fu *et al.* indicate that CS-based films are effective in reducing oxidative stress and the production of reactive oxygen species in fruits.[46] This is accomplished by reducing the impact of UV light on the fruit and the production of reactive oxygen species. This process diminishes the MDA accumulation, thereby extending the fruit's storage life.

Cell membrane permeability, as indicated by relative conductivity, reflects the degree of cell membrane damage in fruits and correlates positively with the fruit freshness. This permeability tends to increase over time during storage.

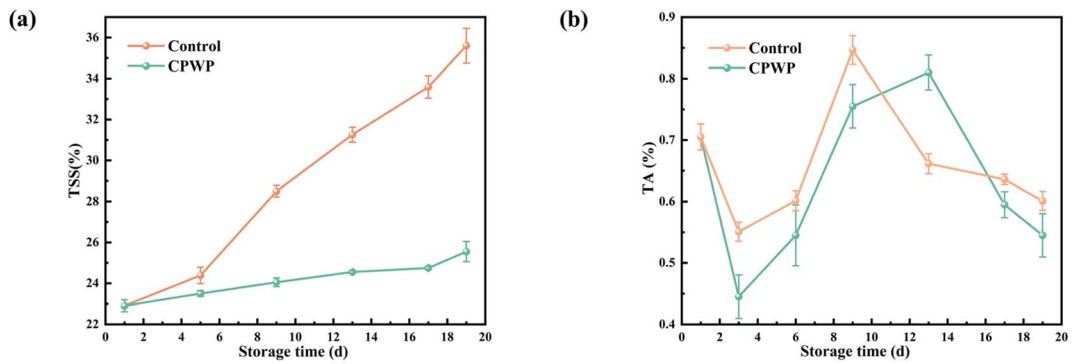

Fig. 9 (a) TSS and (b) TA contents of wolfberries over time.

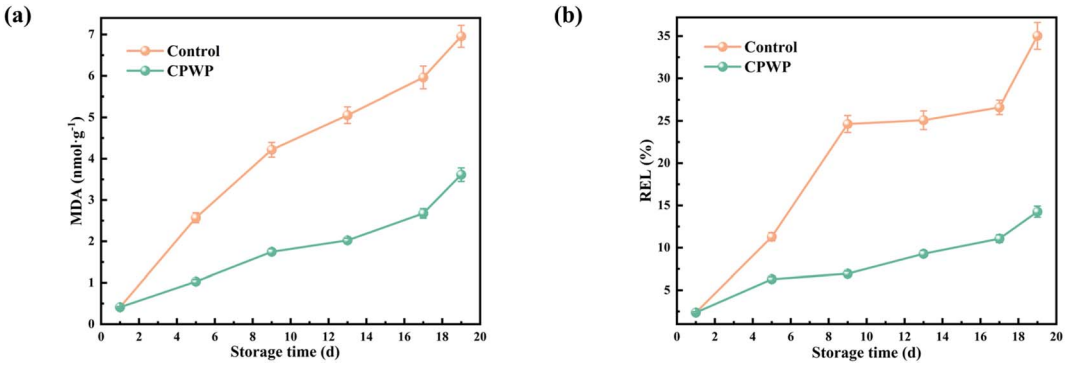

Fig. 10 (a) MDA and (b) REL of wolfberries over time.

Fig. 10(b) presents the changes in the relative conductivity of *Lycium barbarum* stored at 4 °C. The results demonstrate that the relative conductivities of the control and CPWP increased faster in the pre-storage period and more slowly in the late storage period. CPWP was consistently lower than the control, indicating reduced damage to *Lycium barbarum* cell membranes in CPWP, consistent with the observed fruit appearance.

4. Conclusion

A new double-layer packaging film was successfully prepared by adding grapefruit essential oil to the CS/PVA film and coating it onto a PET film. The TG and DTG results showed that the thermal stability of the CS/PVA films loaded with white round grapefruit essential oil was improved. The SEM images showed that the bilayers filled the voids in the CS/PVA films, and the cross-sectional images revealed that the bilayers were tightly connected without delamination. In addition, the WVP and OP of the bilayer film were reduced. The application of the bilayer film on wolfberry packaging was found to extend the shelf life of wolfberries up to 19 days, effectively reduce the weight loss rate, decay rate, and malondialdehyde content of wolfberry, and maintain the titratable acidity, soluble solid content, and relative conductivity changes of wolfberry.

This indicates that the prepared bilayer film showed excellent packaging potential and is expected to be applied to other fruit and vegetable packaging. It is worth noting that the prepared inner layer film is a green film, which can be completely degraded over time. The presence of the outer film not only delays the release of essential oils but also provides excellent barrier and mechanical properties, which can be reused in fruit and vegetable packaging to meet the environmental requirements. In conclusion, the developed CS/PVA-PET bilayer film loaded with essential oils has a promising application in food packaging. The future research goal is to prepare more environmentally friendly and efficient packaging films.

Data availability

Some or all data, models, or code that support the findings of this study are available from the corresponding author upon reasonable request. All data, models, and code generated or used during the study are included in the submitted article.

Author contributions

Mengyun Liu: conceptualization, data curation, investigation, formal analysis, validation, visualization, and writing–original draft. Liuxin Shi: conceptualization, methodology, supervision, writing–review & editing, project administration, and resources. Xiao Zhang: data curation, formal analysis, and software. Yunfeng Zhang: visualization, validation, funding acquisition, and supervision.

Conflicts of interest

There are no conflicts of interest to declare.

Acknowledgements

The authors sincerely thank the testing support from the Advanced Analysis and Testing Centre of Nanjing Forestry University for this study. The authors would also like to acknowledge the GC-MS analysis provided by zkec (**http://www.zkec-c.cc/**).

References

1 Y. Chen, C. Huang, Z. Miao, Y. Gao, Y. Dong, K. C. Tam and H.-Y. Yu, *ACS Nano*, 2024, **18**(12), 8754–8767, DOI: **10.1021/acsnano.3c11335**.
2 B. Wu, S. Y. H. Abdalkarim, Z. Li, W. Lu and H.-Y. Yu, *Carbohydr. Polym.*, 2025, **351**, 123118, DOI: **10.1016/j.carbpol.2024.123118**.
3 M. Mujtaba, R. E. Morsi, G. Kerch, M. Z. Elsabee, M. Kaya, J. Labidi and K. M. Khawar, *Int. J. Biol. Macromol.*, 2019, **121**, 889–904, DOI: **10.1016/j.ijbiomac.2018.10.109**.
4 M. Azmana, S. Mahmood, A. R. Hilles, A. Rahman, M. A. Bin Arifin and S. Ahmed, *Int. J. Biol. Macromol.*, 2021, **185**, 832–848, DOI: **10.1016/j.ijbiomac.2021.07.023**.
5 N. Limpan, T. Prodpran, S. Benjakul and S. Prasarpran, *Food Hydrocolloids*, 2012, **29**, 226–233, DOI: **10.1016/j.foodhyd.2012.03.007**.

6 Z. Yu, B. Li, J. Chu and P. Zhang, *Carbohydr. Polym.*, 2018, **184**, 214–220, DOI: 10.1016/j.carbpol.2017.12.043.
7 H. Falleh, M. Ben Jemaa, M. Saada and R. Ksouri, *Food Chem.*, 2020, **330**, DOI: 10.1016/j.foodchem.2020.127268.
8 Z. Wei, L. Huang, X. Feng, F. Cui, R. Wu, Q. Kong, K. Sun, J. Gao and J. Guo, *Int. J. Biol. Macromol.*, 2023, **253**, DOI: 10.1016/j.ijbiomac.2023.127257.
9 G. J. Lee, S. Y. Lee, N.-G. Kang and M. H. Jin, *LWT-Food Sci. Technol.*, 2022, **160**, DOI: 10.1016/j.lwt.2022.113297.
10 Z. Yang, G. Chen, C. Zhou, Q. Pan, Z. He, C. Wang, Y. Liu, S. Song, L. Yu, Y. Qu and P. Li, *Carbohydr. Polym.*, 2023, 120290, DOI: 10.1016/j.carbpol.2022.120290.
11 S. Li, L. Liu, S. Yang, X. Wang, Y. Yuan, T. Yue, R. Cai and Z. Wang, *Food Hydrocoll.*, 2025, **158**, 110559, DOI: 10.1016/j.foodhyd.2024.110559.
12 F. Wu, M. Misra and A. K. Mohanty, *Prog. Polym. Sci.*, 2021, **117**, 101395, DOI: 10.1016/j.progpolymsci.2021.101395.
13 Z. Lei, X. Chen, F. Cao, Q. Guo and J. Wang, *Int. J. Food Sci. Technol.*, 2022, **57**, 1451–1461, DOI: 10.1111/ijfs.15507.
14 H. Amagase and N. R. Farnsworth, *Food Res. Int.*, 2011, **44**, 1702–1717, DOI: 10.1016/j.foodres.2011.03.027.
15 J. Lamarra, S. Rivero and A. Pinotti, *Int. J. Biol. Macromol.*, 2020, **146**, 811–820, DOI: 10.1016/j.ijbiomac.2019.10.049.
16 E. Velickova, E. Winkelhausen, S. Kuzmanova, V. D. Alves and M. Moldao-Martins, *LWT–Food Sci. Technol.*, 2013, **52**, 80–92, DOI: 10.1016/j.lwt.2013.02.004.
17 N. Roshandel-hesari, M. Mokaber-Esfahani, A. Taleghani and R. Akbari, *Food Chem.*, 2022, **396**, DOI: 10.1016/j.foodchem.2022.133650.
18 Y. Li, L. Han, B. Wang, J. Zhang and J. Nie, *Sci. Hortic.*, 2022, **300**, 111053, DOI: 10.1016/j.scienta.2022.111053.
19 L.-L. Chen, W. Shan, D.-L. Cai, J.-Y. Chen, W.-J. Lu, X.-G. Su and J.-F. Kuang, *Sci. Hortic.*, 2021, **287**, DOI: 10.1016/j.scienta.2021.110264.
20 J. D. C. Santos, E. Coelho, R. Silva, C. P. Passos, P. Teixeira, I. Henriques and M. A. Coimbra, *Ind. Crops Prod.*, 2019, **137**, 541–548, DOI: 10.1016/j.indcrop.2019.05.058.
21 F. Deba, T. D. Xuan, M. Yasuda and S. Tawata, *Food Control*, 2008, **19**, 346–352, DOI: 10.1016/j.foodcont.2007.04.011.
22 E. I. Lucini, M. P. Zunino, M. L. Lopez and J. A. Zygadlo, *J. Phytopathol.*, 2006, **154**, 441–446, DOI: 10.1111/j.1439-0434.2006.01126.x.
23 D. Yu, S. Y. H. Abdalkarim, M. Jin, Y. Zhang and H.-Y. Yu, *Int. J. Biol. Macromol.*, 2025, **286**, 138295, DOI: 10.1016/j.ijbiomac.2024.138295.
24 J. F. Mendes, L. B. Norcino, H. H. A. Martins, A. Manrich, C. G. Otoni, E. E. N. Carvalho, R. H. Piccoli, J. E. Oliveira, A. C. M. Pinheiro and L. H. C. Mattoso, *Food Hydrocolloids*, 2020, **100**, DOI: 10.1016/j.foodhyd.2019.105428.
25 L. Yan, S. Y. H. Abdalkarim, X. Chen, Z. M. Chen, W. Lu, J. Zhu, M. Jin and H.-Y. Yu, *Compos. Sci. Technol.*, 2024, **245**, 110364, DOI: 10.1016/j.compscitech.2023.110364.
26 S. Valizadeh, M. Naseri, S. Babaei, S. M. H. Hosseini and A. Imani, *Int. J. Biol. Macromol.*, 2019, **134**, 604–612, DOI: 10.1016/j.ijbiomac.2019.05.071.
27 H. Chen, X. Hu, E. Chen, S. Wu, D. J. McClements, S. Liu, B. Li and Y. Li, *Food Hydrocolloids*, 2016, **61**, 662–671, DOI: 10.1016/j.foodhyd.2016.06.034.
28 J. Liu, S. Liu, Y. Chen, L. Zhang, J. Kan and C. Jin, *Food Hydrocolloids*, 2017, **71**, 176–186, DOI: 10.1016/j.foodhyd.2017.05.019.
29 W. Lan, S. Wang, M. Chen, D. E. Sameen, K. Lee and Y. Liu, *Int. J. Biol. Macromol.*, 2020, **145**, 722–732, DOI: 10.1016/j.ijbiomac.2019.12.230.
30 T. Erceg, N. Vukic, O. Sovljanski, A. Stupar, V. Sergelj, M. Acimovic, S. Balos, J. Ugarkovic, D. Suput, S. Popovic and S. Rakic, *ACS Sustainable Chem. Eng.*, 2022, **10**, 9141–9154, DOI: 10.1021/acssuschemeng.2c02009.
31 L. Wang, F. Liu, Y. Jiang, Z. Chai, P. Li, Y. Cheng, H. Jing and X. Leng, *J. Agric. Food Chem.*, 2011, **59**, 12411–12419, DOI: 10.1021/jf203165k.
32 M. A. da Silva, A. C. Krause Bierhalz and T. G. Kieckbusch, *Drying Technol.*, 2012, **30**, 72–79, DOI: 10.1080/07373937.2011.620727.
33 V. M. Bispo, A. A. P. Mansur, E. F. Barbosa-Stancioli and H. S. Mansur, *J. Biomed. Nanotechnol.*, 2010, **6**, 166–175, DOI: 10.1166/jbn.2010.1110.
34 J. Ding, R. Zhang, S. Ahmed, Y. Liu and W. Qin, *Molecules*, 2019, **24**, DOI: 10.3390/molecules24071408.
35 Y. Chen, Y. Li, S. Qin, S. Han and H. Qi, *Composites, Part B*, 2022, **238**, DOI: 10.1016/j.compositesb.2022.109868.
36 Z. Li, X. Jiang, H. Huang, A. Liu, H. Liu, N. Abid and L. Ming, *Int. J. Biol. Macromol.*, 2022, **208**, 983–994, DOI: 10.1016/j.ijbiomac.2022.03.200.
37 Y. Peng and Y. Li, *Food Hydrocolloids*, 2014, **36**, 287–293, DOI: 10.1016/j.foodhyd.2013.10.013.
38 X.-L. Li, Y. Shen, F. Hu, X.-X. Zhang, K. Thakur, K. R. R. Rengasamy, M. R. Khan, R. Busquets and Z.-J. Wei, *Int. J. Biol. Macromol.*, 2023, **242**, DOI: 10.1016/j.ijbiomac.2023.124767.
39 P. Tongnuanchan, S. Benjakul and T. Prodpran, *Food Sci. Technol.*, 2013, **48**, 2143–2149, DOI: 10.1111/ijfs.12198.
40 F. Ebrahimi and S. Rastegar, *Sci. Hortic.*, 2020, **265**, DOI: 10.1016/j.scienta.2020.109258.
41 W. Xiang, H.-W. Wang, Y. Tian and D.-W. Sun, *J. Food Process Eng.*, 2021, **44**, DOI: 10.1111/jfpe.13764.
42 Z. Yang, C. Guan, C. Zhou, Q. Pan, Z. He, C. Wang, Y. Liu, S. Song, L. Yu, Y. Qu and P. Li, *Carbohydr. Polym.*, 2023, **300**, DOI: 10.1016/j.carbpol.2022.120290.
43 C. Pelayo, S. E. Ebeler and A. A. Kader, *Postharvest Biol. Technol.*, 2003, **27**, 171–183, DOI: 10.1016/s0925-5214(02)00059-5.
44 O. B. Sogvar, M. K. Saba and A. Emamifar, *Postharvest Biol. Technol.*, 2016, **114**, 29–35, DOI: 10.1016/j.postharvbio.2015.11.019.
45 D. Zhou, Q. Zhang, C. Wu, T. Li and K. Tu, *Sci. Hortic.*, 2022, **295**, DOI: 10.1016/j.scienta.2021.110863.
46 X. Fu, X. Chang, S. Xu, H. Xu, S. Ge, Y. Xie, R. Wang, Y. Xu, Z. Luo, Y. Shan and S. Ding, *Int. J. Biol. Macromol.*, 2024, **254**, DOI: 10.1016/j.ijbiomac.2023.127968.